

## Coagulation performance of a novel poly-ferric-acetate (PFC) coagulant in phosphate-kaolin synthetic water treatment

Yanxin Wei<sup>\*,†</sup>, Jinpeng Lu<sup>\*</sup>, Xiongzi Dong<sup>\*</sup>, Jianwen Hao<sup>\*\*</sup>, and Chengli Yao<sup>\*</sup>

<sup>\*</sup>College of Chemistry and Chemical Engineering, Hefei Normal University, Hefei 230061, China

<sup>\*\*</sup>Department of Chemical Engineering, Anhui Vocational and Technical College, Hefei 230051, China

(Received 25 December 2016 • accepted 8 July 2017)

**Abstract**—The process of coagulation-flocculation is increasingly applied in wastewater treatment. And the polymerized inorganic coagulants are widely used among these coagulation-flocculation processes. However, conventional coagulants using sulfates or chlorides as counter anion may give rise to corrosion. The purpose of this study was to synthesize PFC coagulants in which acetate is used as counter anion. The influences on the preparation of PFC were optimized. The synthesis was done at the optimum conditions, such as temperature of 60 °C, the Fe/CH<sub>3</sub>COOH molar ratio of 1 : 4.0 and reaction time of 6 h, respectively. The prepared PFC coagulants were characterized by Fourier transform infrared (FTIR) spectrophotometry and scanning electron microscopy (SEM). PFC was found to mainly form complexation polymeric species and present more cluster and lamellar structure. A series of jar tests were carried out to study the coagulation performance of PFC and PFS in phosphate-kaolin synthetic water treatment. Results showed that the coagulation performance of PFC was more efficient than PFS's in terms of the phosphorus removal efficiency and the residual turbidity. Due to using acetate as counter anion to iron, PFC is less harmful to the processes of water treatment and equipment than that of the conventional coagulants applied chlorides or sulfates. Therefore, PFC is a promising coagulant in the process of corrosion sensitive applications and the process of wastewater containing phosphorus treatment.

Keywords: Poly-ferric-acetate, Coagulation Performance, Phosphorus, Wastewater Treatment

### INTRODUCTION

With the development of urbanization, industrialization and agriculture, many nutrients of phosphorus are discharged into water, posing a serious threat to the aquatic ecosystem. Even though phosphorus is a beneficial element in the ecosystem, the excess phosphorus in fresh water body will cause eutrophication [1]. Especially, compounds of phosphorus can be assimilated by algae and plants and then lead to blooms of algae and plants. Consequently, the balance of organisms and quality of the water are damaged. Owing to the environmental problem of eutrophication, many countries have developed more stringent regulations on the phosphorus discharge limits in effluents [2,3]. Therefore, the removal of phosphorus has been studied for decades [4-7]. To reduce the concentration of phosphorus in wastewater, physical, chemical and biological processes have been developed [5,7-9]. Among these, coagulation-flocculation (CF) is one of the most vital and common chemical treatment processes used in wastewater treatment plant due to its simple operation, low capital cost and environmental impact [10,11].

Many studies have been developed to improve the performance of the coagulation-flocculation process [12-16]. One of the general coagulants used in the coagulation/flocculation process is the Al and Fe-based coagulants. Although aluminum-based coagulants are widely used, iron-based coagulants are favorable options in

many applications. A major drawback of aluminum applications is their potential contribution to Alzheimer's disease [17]. Thus the processes of water treatment using iron based coagulants have been extensively studied lately [11,18-23]. The coagulation performance of the most common iron salts, namely prehydrolyzed polyferric sulphates and polyferric chlorides have been widely studied in various wastewater treatment. Except for the most common coagulants, some new iron-based coagulants are synthesized, for example, polyferric silicate sulfate (PFSIS) [24].

The iron-based coagulants used in the process of water treatment are mostly sulfates and chlorides. These counter anions may produce different problems in different applications. For example, chloride may give rise to corrosion. Not only steel constructions but also concrete and aluminum are corroded. Except for chloride, sulfate may also cause corrosion on various materials [25]. Acetate may be an alternative to these counter anions because it is less corrosive than chloride or sulfate.

We used the anion of acetic acid, acetate [CH<sub>3</sub>COO<sup>-</sup>] to replace the harmful counter SO<sub>4</sub><sup>2-</sup> and Cl<sup>-</sup> that are commonly used in iron-based coagulants. A novel composite coagulant polyferric-acetate was prepared by using FeSO<sub>4</sub>·7H<sub>2</sub>O and acetic acid. First, the Fe/CH<sub>3</sub>COOH molar ratio (n), preparation temperature and reaction time on coagulation performance were studied systematically. Second, its structure was analyzed with Fourier transform infrared (FTIR) spectrophotometer, and its surface morphology was investigated with scanning electron microscopy (SEM). Finally, the influences such as the coagulant dosage, the initial wastewater pH and the settling time on the coagulation performance of PFC were also

<sup>†</sup>To whom correspondence should be addressed.

E-mail: yxwei73@mail.ustc.edu.cn

Copyright by The Korean Institute of Chemical Engineers.

studied in terms of the residual turbidity and the phosphorus removal efficiency. And then the coagulation performance of PFC was compared with common coagulant, namely PFS.

## MATERIALS AND METHODS

### 1. Preparation of Coagulant

All reagents used for the preparation of PFC were analytical reagent. Deionized water was used to prepare all working solutions. The coagulant samples of PFC were synthesized at suitable temperature. First, the pre-determined amount of acetic acid solution, varying with the Fe/CH<sub>3</sub>COOH molar ratio (n), was slowly added to FeSO<sub>4</sub> solution under agitation. The n values in this study were selected in the range of 1 : 4.5-1 : 2.5. Then, the liquid mixture was placed in an electro thermostatic water bath (Jintan Langbo Instrument manufacturing Co. Ltd., China). According to the amount of Fe<sup>2+</sup>, the calculated potassium chlorate was gradually added into the reaction vessel and oxidate the Fe(II) to Fe(III). Temperature was varied in the range of 40 °C-70 °C for optimization purpose. A new liquid mixture was formed and kept in electro thermostatic water bath at a pre-determined temperature for reaction time. Finally, PFC was obtained.

### 2. Structure and Morphology

The liquid samples of PFC and PFS were dried in an oven at 50 °C for several days and then ground into powder. The powders of PFC and PFS were analyzed by using potassium bromide (KBr) pellet with the Nicolet-380 FTIR Spectrophotometer. The spectra varied in the range of 4,000-400 cm<sup>-1</sup>. Then the surface morphology of the coagulants was observed using a scanning electron microscope (SEM). The SEM and EDX analysis was performed using model SU1510, with an X-ray detector of energy dispersion.

### 3. Wastewater Preparation and Chemical Analysis

The predetermined amount of kaolin (chemically pure) was dissolved in deionized water to obtain 0.2 g/L kaolin solution, and then the proper amount of potassium dihydrogen phosphate was added to this suspension. The main characteristics of the synthetic wastewater are shown in Table 1. According to [26,27], the total

**Table 1. Characteristics of the synthetic wastewater**

Parameter	Unit	Value
pH	-	7.76
Turbidity	NTU	291.7
Total phosphorus concentration	mg/L	5.06

phosphorus (TP) concentration was determined by using ammonium molybdate spectrophotometric method. The turbidity was determined by spectrophotometric method. The concentration of TP and the turbidity in the water sample were measured by using a model 722E spectrophotometer (Shanghai Yuanxi Instrument Ltd., China). As shown in Fig. 1, the absorbance in the water sample varied linearly with the TP concentration and turbidity. The coefficients of determination (R<sup>2</sup>) values were 0.9999. The linearity in both cases confirms the validity of the methods. In the case of higher TP concentrations and turbidity, the samples were first diluted before the determination of concentration and turbidity in a similar manner.

### 4. Jar Test Procedure

Coagulation-flocculation experiments were carried out using synthetic wastewater containing phosphorus in 500 mL beakers. The jar tests were conducted using stirring apparatus (Model RH-6, Changzhou Renhe Instrument factory, China). After adding the coagulant into the water samples, rapid mixing at 250 rpm was applied for 2 min; the mixing speed was lowered to 60 rpm for a duration of 15 min. Then after 20 min of quiescent settling, water samples were collected from 2 cm under the water surface for TP concentration and turbidity measurement. Note that the coagulant dosage was calculated as mg Fe/L.

### 5. Calculation of the Phosphorus Removal Efficiency

The phosphorus removal efficiency (RP%) was calculated in Eq. (1)

$$RP(\%) = \frac{C_0 - C_t}{C_0} \times 100 \quad (1)$$

where C<sub>0</sub> is the initial TP concentration of the synthetic wastewa-

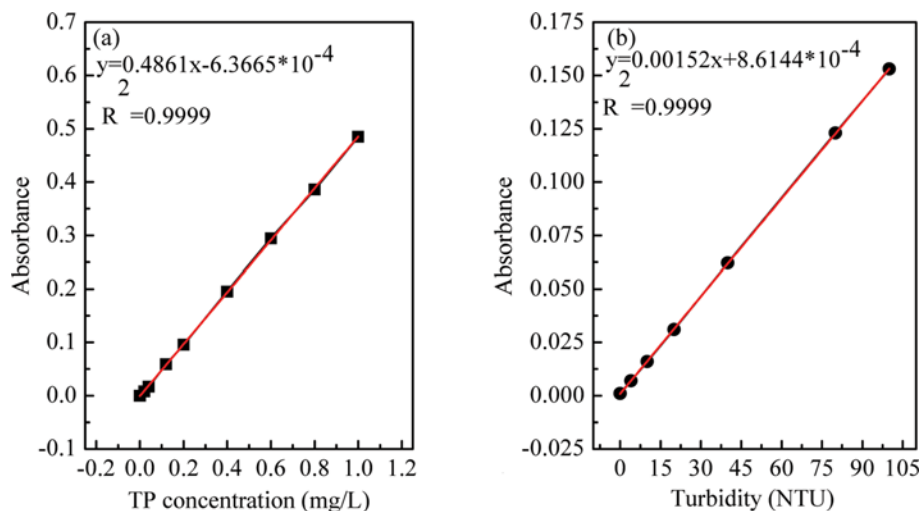


**Fig. 1. Plot of TP concentration and turbidity versus absorbance.**

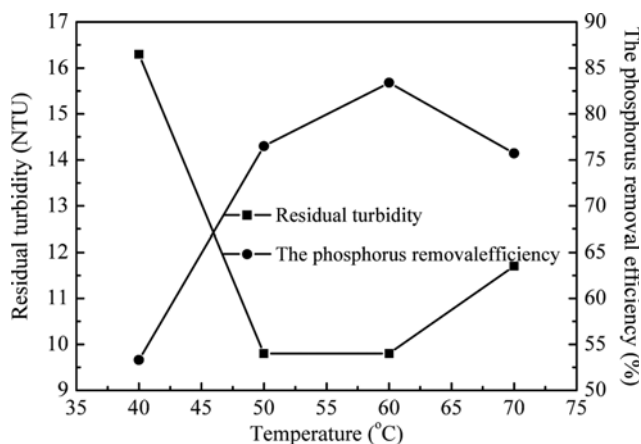


Fig. 2. Effect of temperature on the coagulation performance of PFC.

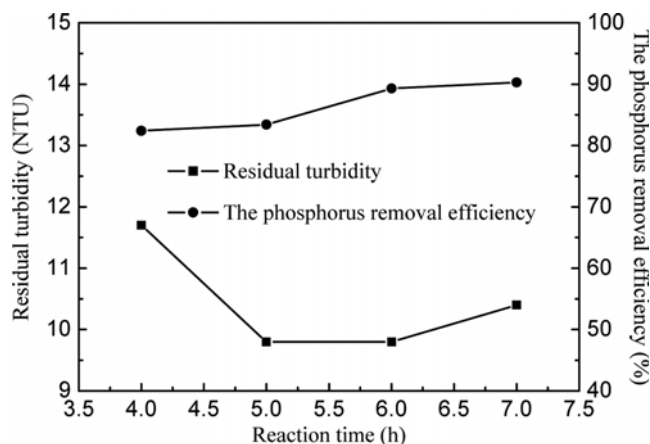


Fig. 3. Effect of reaction time on the coagulation performance of PFC.

ter;  $C_t$  is the TP concentration of the water sample collected at the end of a predetermined settling time ( $t$ ) after the coagulation run.

## RESULTS AND DISCUSSION

### 1. Preparation of PFC

In the preparation of PFC, there are many experimental parameters affecting the coagulant-flocculation performance of PFC. To obtain the optimum experimental parameters, the different experiment parameters, such as Fe/CH<sub>3</sub>COOH molar ratios ( $n$ ), temperature, and reaction time, were varied.

#### 1-1. Effect of the Temperature

To investigate the effect of temperature, the reaction time and Fe/CH<sub>3</sub>COOH molar ratio were kept constant at 5.0 h and 1:4.5, respectively, while the temperature was varied between 40 °C-70 °C. Fig. 2 shows the effect of the temperature on the coagulation performance of PFC. The residual turbidity was observed to decrease with an increase in the temperature in the range of 40 °C-60 °C. Subsequently, the residual turbidity increased slightly while increasing the temperature from 60 °C to 70 °C. The efficiencies of phosphorus removal increased as the temperature increased at the beginning, but showed a decreasing trend afterwards. Generally, at higher temperature, the extent of the polymerization formed by the hydrolyzing Fe(III) was greater, leading to stronger charge neutralization and adsorption-bridging capacity of PFC, thus improving coagulation-flocculation performance. However, the hydrolyzation and sedimentation of Fe<sup>3+</sup> will become strong if the temperature is too high, which causes the coagulation performance of PFC to become bad. This explains the fact that the trend of the phosphorus removal efficiency curve increases at the beginning and decreases afterwards; the trend of residual turbidity curve decreases at the beginning and increases afterwards. Furthermore, much energy is needed for preparing PFC with the increase of temperature, which will prevent the industrial preparation of PFC. Consequently, 60 °C was chosen as the optimum temperature of PFC preparation.

#### 1-2. Effect of the Reaction Time

To determine the effect of reaction time, the temperature and Fe/CH<sub>3</sub>COOH molar ratio were kept constant at 60 °C and 1:4.5,

respectively, while the reaction time was varied. Fig. 3 shows the effect of the reaction time on the coagulation performance of PFC. The residual turbidity decreased with increase of reaction time, followed by a slight increase. When it comes to the phosphorus removal efficiency curve, there is increase in the phosphorus removal efficiency at the beginning but an unobvious trend of increase afterwards. The residual turbidity decreases and the phosphorus removal efficiency increases at the beginning, indicating that the basicity ( $B$ ) of PFC increases as the reaction time increases. Generally, the higher  $B$  is, the more polymerization extent formed by the hydrolyzing Fe(III) is, which will lead to a increase in charge neutralizing and adsorption-bridging capacity of PFC, thus improving the coagulation performance. As time elapses, the  $B$  of PFC increases above the  $B$  limits, which causes the hydrolyzation and sedimentation of Fe<sup>3+</sup> in the coagulant of PFC to increase. This explains the fact that the residual turbidity increases slightly and the phosphorus removal efficiency has no obvious increase afterwards. Therefore, 6.0 h was chosen as the optimum reaction time.

#### 1-3. Effect of the Fe/CH<sub>3</sub>COOH Molar Ratio ( $n$ )

To discover the effect of Fe/CH<sub>3</sub>COOH molar ratio, the tem-

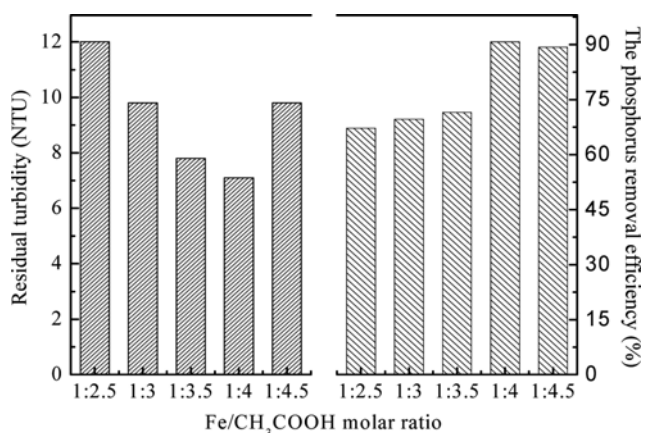


Fig. 4. Effect of the Fe/CH<sub>3</sub>COOH molar ratio on the coagulation performance of PFC.

perature and reaction time were kept constant at 60 °C and 6 h, respectively, while the Fe/CH<sub>3</sub>COOH molar ratio was varied. Fig. 4 shows effect of the Fe/CH<sub>3</sub>COOH molar ratio on the coagulation performance of PFC. The results show that the residual turbidity decreases with the decrease of the Fe/CH<sub>3</sub>COOH molar ratio (from 1 : 2.5 to 1 : 4.0) and increases subsequently. As far as the phosphorus removal efficiency is concerned, the phosphorus removal efficiency increases with the decrease of the Fe/CH<sub>3</sub>COOH molar ratio (from from 1 : 2.5 to 1 : 4.0) and slightly decreases subsequently. The main reasons are as follows: the low value of the Fe/CH<sub>3</sub>COOH molar ratio leads to a high concentration of CH<sub>3</sub>COOH, which increases the H<sup>+</sup> in the solution and thus limits the basicity (B) at a suitable range of B. However, the concentration of CH<sub>3</sub>COOH is too low; B is too high and even extends beyond the B limit, resulting in an increase in hydrolyzation and sedimentation of Fe<sup>3+</sup>, which worsens the coagulation performance of PFC. On the contrary, the concentration of CH<sub>3</sub>COOH is too high, and B may become low, which causes the hydrolyzation of Fe(III) to become more difficult and less polymerization extent of PFC to form, thus worsening the coagulation performance. Therefore, 1 : 4.0 was considered as the optimum Fe/CH<sub>3</sub>COOH molar ratio.

## 2. Structure and Morphology

### 2-1. FT-IR Spectroscopy

Fig. 5 shows the FT-IR spectra of the PFC and PFS. The peaks at the range of 3,500-3,200 cm<sup>-1</sup> for both PFC and PFS (3,429 cm<sup>-1</sup> for PFC and 3,381 cm<sup>-1</sup> for PFS) are assigned to the intermolecular association stretching vibration of -OH [28]. The medium peaks at range of 1,640-1,632 cm<sup>-1</sup> (1,636 cm<sup>-1</sup> for PFC and 1,634 cm<sup>-1</sup> for PFS) can be attributed to the bending vibration of water [29]. And this indicates that PFC and PFS may contain structural and adsorbed water. In addition, the peaks at 535, 472 cm<sup>-1</sup> for PFC and 466, 598 cm<sup>-1</sup> for PFS are related to the stretching vibration of Fe-O, respectively [30]. There is a significant difference in the spectra of PFC and PFS. The peak at 1,130 cm<sup>-1</sup> is assigned to the SO<sub>4</sub><sup>2-</sup> stretching vibration [12], which is only presented in PFS. The peaks at 2,922, 2,855 cm<sup>-1</sup> for PFC are assigned to the C-H stretching vibration in the methyl. The peak at 1,423 cm<sup>-1</sup> can be attributed to the bending vibration of C-H in the methyl. And this indicates

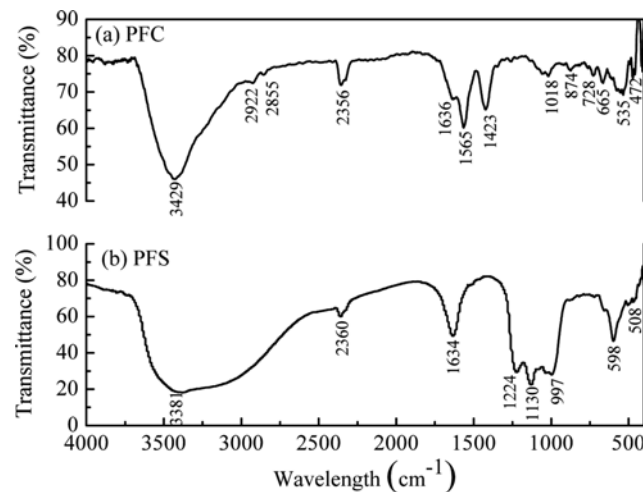


Fig. 5. Infrared spectrum: (a) PFC and (b) PFS.

that PFC contains structural methyl. The PFC curve shows the presence of absorption at peaks of 1,018 and 874 cm<sup>-1</sup>, indicating the presence of C-C stretching vibration. The peak at 665 cm<sup>-1</sup> for PFC is related to the structure of -COO.

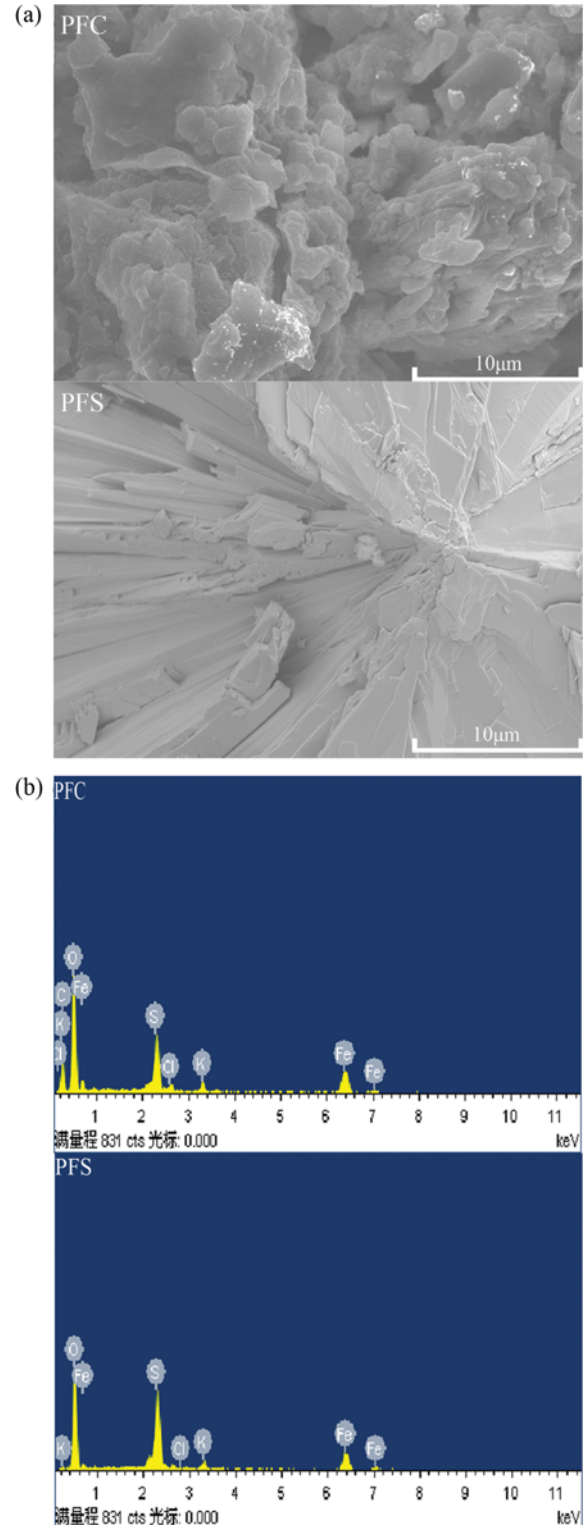


Fig. 6. SEM images and EDX analysis: (a) SEM images and (b) EDX analysis.

## 2-2. SEM and EDX Results

The surface morphology of PFC and PFS was investigated by applying scanning electron microscopy (SEM). Fig. 6(a) shows the SEM photographs of PFC and PFS. It can be seen that the surface of PFC is formed more cluster and lamellar than PFS's surface which is smooth. The molecular cluster and lamellar structure of PFC are connected to promotion of the adsorption and bridging ability of PFC. Fig. 6(b) shows the EDX spectrum of PFC and PFS, respectively. As determined by EDX, the element of C is presented in PFC. It shows that major elements of PFC are C, Fe, O, S, and of PFS are Fe, O, S.

## 3. Evaluation of PFC

To evaluate the coagulation performance of PFC which was prepared at optimum conditions, it was applied in the treatment of synthetic wastewater and compared with conventional coagulant of PFS.

### 3-1. Effect of Coagulant Dosage on the Phosphorus Removal Efficiency and the Residual Turbidity

Fig. 7 shows the effect of coagulant dosage on the phosphorus removal efficiency and the residual turbidity in the treatment of synthetic wastewater. As shown in Fig. 7(a), PFC and PFS achieve the

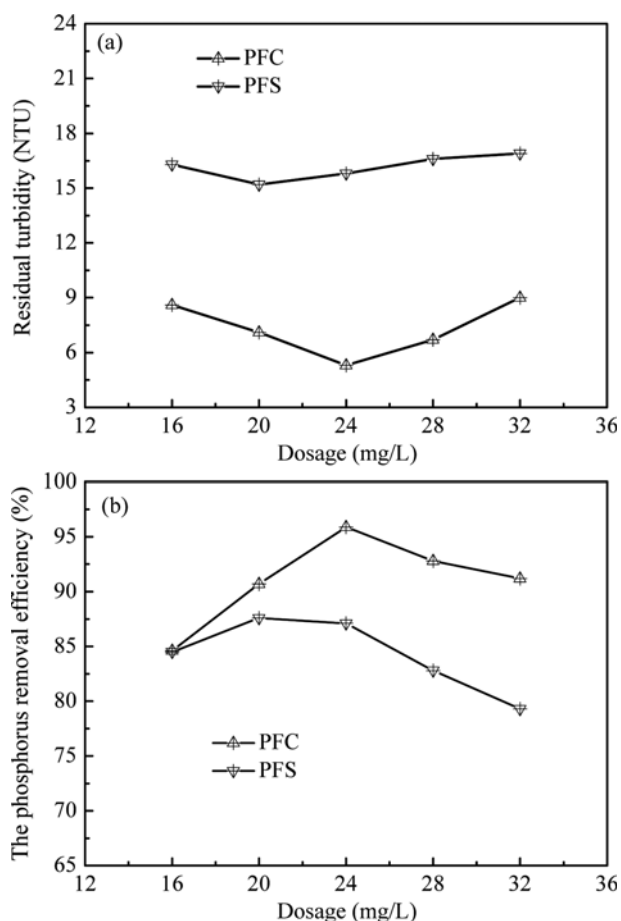


Fig. 7. Effect of coagulant dosage. (a) the residual turbidity of water samples and (b) the phosphorus removal efficiency of water samples. The other operation conditions were initial synthetic wastewater pH=7.76, the settling time=20 min.

lowest residual turbidity 5.3 and 15.2 NTU at the coagulant dosage of 24 and 20 mg/L, respectively, while the residual turbidity decreases with increase of the coagulant dosage at the beginning and increases afterwards. Fig. 7(b) indicates that both the phosphorus removal efficiency curves reveal an increasing trend with increase of coagulant dosage. Subsequently, as the coagulant increases, the phosphorus removal efficiency decreases in both curves. Logically, it is true, the higher coagulant dosage, the stronger charge neutralization and adsorption-bridging ability of PFC and PFS. However, with the dosages further increased, PFC and PFS coagulants will produce more flocs with positive charges. It leads to the result that the redundant flocs with positive charges can be adhered to the surface of aggregates. This may be the reason for the high residual turbidity and low phosphorus removal efficiency in the latter part of coagulant dosage range due to charge repulsion among the particles with similar charges. There is an apparent lower residual turbidity and higher phosphorus removal efficiency of PFC than that of PFS within the coagulant dosage range. SEM images show that PFC's structure is more cluster and lamellar than PFS's, which is more helpful in neutralizing charge and forming bridge-aggregation among the colloidal particles in synthetic wastewater.

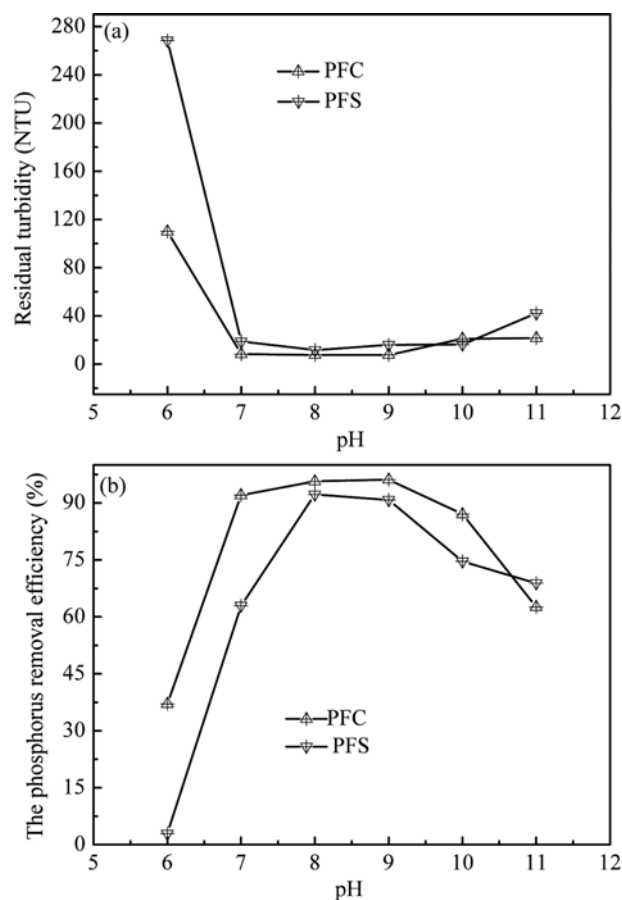


Fig. 8. Effect of initial synthetic wastewater pH. (a) the residual turbidity of water samples and (b) the phosphorus removal efficiency of water samples. The other operation conditions were the PFC dosage=24 mg/L, the PFS dosage=20 mg/L, the settling time=20 min.

### 3-2. Effect of Initial Synthetic Wastewater pH on the Phosphorus Removal Efficiency and the Residual Turbidity

Fig. 8 shows the effects of initial synthetic wastewater pH on the phosphorus removal efficiency and the residual turbidity in the treatment of synthetic wastewater. The value of pH is adjusted by applying 0.1 mol/L NaOH and 0.1 mol/L HCl. In both cases, the residual turbidity decreases and the phosphorus removal efficiency increases as the pH increases from 6 to 8. However, the residual turbidity increases slightly and the phosphorus removal efficiency decreases with increase of the pH from 8 to 11. The main reasons are as follows:  $\text{OH}^-$  increases with pH increasing, more ferrite polymers are produced due to  $\text{OH}^-$  reacts with the Fe species, and the higher ability of the bridging flocculation is enhanced. At the same time, the colloids particle charges are reduced because of the charge neutralization increasing, which may enhance the destabilization of the colloidal particles in wastewater. However, at higher pH, the coagulant will be susceptible to hydrolysis, which can inhibit the bridging flocculation. Therefore, the coagulation performance can reach maximum at an optimum pH value. At optimal pH value in the range of 7-9, PFC can reach the minimum residual turbidity

of 5.3 NTU, and the maximum phosphorus removal efficiency is 96.1%; whereas PFS can only reach the residual turbidity of 11.7 NTU, and the highest phosphorus removal efficiency was 92.2%.

### 3-3. Effect of Settling Time on the Phosphorus Removal Efficiency and the Residual Turbidity

Fig. 9 shows the effect of settling time on the phosphorus removal efficiency and the residual turbidity in the treatment of synthetic wastewater. The flocs hydrolyzed by PFC settle quickly, the phosphorus removal efficiency achieves over 94%, and the residual turbidity can reach 12.0 NTU at settling time of 5 min, in comparison with 35 min for PFS. The main reason is that PFC samples have more strongly and tightly the charge neutralization and bridge-flocculation of amongst flocs than PFS. Additionally, the structure and the surface morphology of PFC coagulant have been influenced by the  $\text{CH}_3\text{COO}^-$ , which is more advantageous to coagulate colloidal particles and form bridging-aggregation among flocs in synthetic wastewater. Thus, the coagulation performance of PFC has better efficiency than that of PFS. It is also clearly noticed that the residual turbidity and the phosphorus removal efficiency for PFC and PFS has slightly decreasing and increasing tendency after settling 20 min.

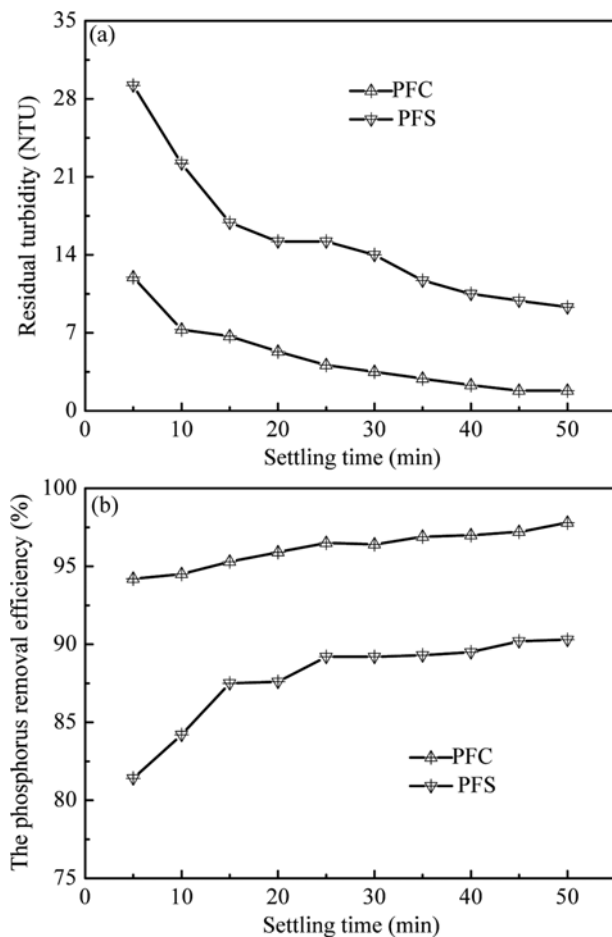


Fig. 9. Effect of settling time. (a) the residual turbidity of water samples and (b) the phosphorus removal efficiency of water samples. The other operation conditions were the PFC dosage=24 mg/L, the PFS dosage=20 mg/L, initial synthetic wastewater pH=7.76.

## CONCLUSIONS

A novel poly-ferric-acetate coagulant was prepared using  $\text{CH}_3\text{COOH}$  as acidification reagent. The various factors which influence the preparation of PFC were optimized. Optimum conditions for the synthesis were established as follows: temperature of  $60^\circ\text{C}$ , the  $\text{Fe}/\text{CH}_3\text{COOH}$  molar ratio of 1 : 4.0 and a reaction time of 6 h. The structure and coagulation performance of the PFC coagulant were investigated and compared with the conventional coagulant PFS. According to the FTIR results, polymeric complexes were formed. SEM images show that the structure of PFC had more clusters and was more lamellar than the structure of PFS. And then the PFC abilities of coagulating colloidal particles and forming bridge-aggregation among flocs were greatly improved, which led to the better coagulation performance compared with PFS. At optimal pH value in the range of 7-9, PFC can reach the highest phosphorus removal efficiency 96.1% and the lowest residual turbidity 5.3 NTU at the best dosage of 24 mg/L, whereas PFS can only reach the highest phosphorus removal efficiency 92.2% and the lowest residual turbidity 11.7 NTU at the best coagulant dosage of 20 mg/L. Moreover, the acetate as a counter anion to iron is less harmful to the processes of water treatment and equipment than that of the conventional coagulants applied chlorides or sulfates. Therefore, PFC is a promising coagulant in the process of corrosion sensitive applications and the process of wastewater containing phosphorus treatment. Another potential application is that PFC is also used in process of wastewater treatment before biological treatment because the carbon from PFC can be used by denitrification bacteria for its nutrition.

## ACKNOWLEDGEMENTS

This research is supported by the Foundations of Educational Committee of Anhui Province (Nos. KJ2015A181, KJ2015A262,

KJ2015A287, KJ2014A130), the Important Project of Anhui Provincial Education Department (gxyqZD2016229).

## REFERENCES

1. G. D. T. V. H. Smith and J. C. Nekola, *Environ. Pollut.*, **100**, 179 (1999).
2. J. A. Oleszkiewicz and J. L. Barnard, *Water Qual. Res. J. Can.*, **41**, 449 (2006).
3. X. Wei, R. C. Viadero Jr. and S. Bhojappa, *Water Res.*, **42**, 3275 (2008).
4. P. Wilfert, P. S. Kumar, L. Korving, G. J. Witkamp and M. C. van Loosdrecht, *Environ. Sci. Technol.*, **49**, 9400 (2015).
5. J. O. Kim and J. Chung, *KSCE J. Civ. Eng.*, **18**, 956 (2014).
6. A. O. Babatunde, Y. Q. Zhao, Y. Yang and P. Kearney, *Chem. Eng. J.*, **136**, 108 (2008).
7. L. E. de-Bashan and Y. Bashan, *Water Res.*, **38**, 4222 (2004).
8. S. Rasoul-Amini, N. Montazeri-Najafabady, S. Shaker, A. Safari, A. Kazemi, P. Mousavi, M. A. Mobasher and Y. Ghasemi, *Biocatal. Agr. Biotechnol.*, **3**, 126 (2014).
9. A. Beuckels, E. Smolders and K. Muylaert, *Water Res.*, **77**, 98 (2015).
10. A. K. Verma, R. R. Dash and P. Bhunia, *J. Environ. Manage.*, **93**, 154 (2012).
11. T. Chen, B. Gao and Q. Yue, *Colloids Surf., A.*, **355**, 121 (2010).
12. Y. Wei, X. Dong, A. Ding and D. Xie, *J. Taiwan Inst. Chem. E.*, **58**, 351 (2016).
13. Y. X. Zhao, S. Phuntsho, B. Y. Gao, Y. Z. Yang, J. H. Kim and H. K. Shon, *J. Environ. Manage.*, **147**, 194 (2015).
14. C. Wang, A. Alpatova, K. N. McPhedran and M. Gamal El-Din, *J. Environ. Manage.*, **160**, 254 (2015).
15. B. Guo, H. Yu, B. Gao, H. Rong, H. Dong, D. Ma, R. Li and S. Zhao, *Colloids Surf., A.*, **481**, 476 (2015).
16. Y. X. Zhao, B. Y. Gao, Y. Wang, H. K. Shon, X. W. Bo and Q. Y. Yue, *Chem. Eng. J.*, **183**, 387 (2012).
17. J. Li, S. Jiao, L. Zhong, J. Pan and Q. Ma, *Colloids Surf., A.*, **428**, 100 (2013).
18. A. I. Zouboulis, P. A. Moussas and F. Vasilakou, *J. Hazard. Mater.*, **155**, 459 (2008).
19. X. Xu, S. I. Yu, W. Shi, Z. q. Jiang and C. Wu, *Sep. Purif. Technol.*, **66**, 486 (2009).
20. S. Jeong, F. Nateghi, T. V. Nguyen, S. Vigneswaran, Tuan and A. Tu, *Desalination*, **283**, 106 (2011).
21. K. E. Lee, T. T. Teng, N. Morad, B. T. Poh and M. Mahalingam, *Desalination*, **266**, 108 (2011).
22. T. Sun, C. H. Sun, G. L. Zhu, X. J. Miao, C. C. Wu, S. B. Lv and W. J. Li, *Desalination*, **268**, 270 (2011).
23. G. Zhu, H. Zheng, Z. Zhang, T. Tshukudu, P. Zhang and X. Xiang, *Chem. Eng. J.*, **178**, 50 (2011).
24. A. I. Zouboulis and P. A. Moussas, *Desalination*, **224**, 307 (2008).
25. T. E. Graedel, *J. Electrochem. Soc.*, **136**, C204 (1989).
26. G. C. Zhu, Q. Wang, J. Yin, Z. W. Li, P. Zhang, B. Z. Ren, G. D. Fan and P. Wan, *Water Res.*, **201**, 100 (2016).
27. T. J. Park, V. Ampunana, S. Lee and E. Chunga, *Chemosphere*, **2264**, 144 (2016).
28. R. Li, C. He and Y. He, *Chem. Eng. J.*, **223**, 869 (2013).
29. Y. Zeng and J. Park, *Colloids Surf., A.*, **334**, 147 (2009).
30. Y. Fu, S. L. Yu, Y. Z. Yu, L. P. Qiu and B. Hui, *J. Environ. Sci.*, **19**, 678 (2007).